Chapter-4

Synthesis, characterization and application of PVC/Nano-alumina composite membrane

In this chapter, polyvinyl chloride membranes with alumina nanoparticles were prepared via non-solvent induced phase separation method. Membranes were further characterized using High-Resolution Scanning Electron Microscope, Energy-dispersive X-ray spectroscopy EDX, X-ray diffraction, Universal Testing Machine , Thermal Gravimetric Analysis and Drop Shape Analyzer to identify the effect of nanoparticles on the physicochemical properties of PVC composite membranes. To check the effect of nanoparticles on the performance and antifouling nature of composite membranes, some experiments were done on a lab-scale filtration set up for the separation of humic acid from the aqueous humic acid solution. The results were compared for pure PVC and alumina composite membranes in the form of membrane flux, humic acid rejection, fouling ratio, flux recovery and resistance to the separation. The outcome of instrumental analysis of composite membranes and filtration experiments are discussed in detail in this chapter.

4.1 Introduction

Membrane separation processes are gaining high importance among the various available separation processes in the chemical, pharmaceutical and food industries as well as effluent treatment plants and water treatment. This high demand of these processes is due to their advantages over conventional separation process. Some of the advantages are easy and simple mechanism, continuous operation, low energy requirement for separation, operational flexibility, a broad range of separation of solutes

of different size from meso to nano range and high selectivity of membrane material for desired application (Baker, 2012; Lee et al., 2016; Strathman et al., 2006).

However, these separation processes have some limitations also. The major limitation is membrane fouling. A most prominent way to mitigate fouling is to modify the membrane material for increasing its chemical and physical properties. Surface modifications are done by surface coating or plasma treatment while the bulk modification is done either by polymer blending or incorporation of inorganic nanomaterials with the membrane structure (Li et al., 2017; Zhang et al., 2016).

Presently, a lot of studies have been done by various researchers for synthesis of membranes, made of various polymers, such as cellulose acetate (Kim et al., 2019; Rajesha et al., 2019), polytetrafluoroethylene (Feng et al., 2018), polysulfone (Anadão et al., 2010; Kim et al., 2018), polyacrylonitrile (Austria et al., 2019), polyethylene (Zuo et al., 2016), polyvinyl chloride (Behboudi et al., 2016; Farjami et al., 2019; Yong et al., 2019), polyethersulfone (Choudhury et al., 2019; Zhang et al., 2018a) and polyvinylidene fluoride. Many researchers have done studies to prepare porous polymeric mix matrix membranes using many different nanomaterials like titania (Rabiee et al., 2014; Safarpour et al., 2015; Yuliwati et al., 2011), silica (Akbari et al., 2016; Yu et al., 2015), zirconia (Huang et al., 2012; Zhang et al., 2011), alumina (Maximous et al., 2009; Saleh et al., 2012), silver oxide (Mocanu et al., 2019), zinc oxide (Rabiee et al., 2015) etc. to investigate their effect on antifouling properties and performance of the membrane. However, to the best of our knowledge, there is less published information on polyvinyl chloride based composite membranes using alumina nanoparticles to enhance their antifouling properties.

Polyvinyl chloride (PVC) is one of the widely used polymers worldwide for different applications because it is inexpensive, has excellent chemical properties such as acid

and alkali resistance, great mechanical strength and good thermal properties (Zhang et al., 2009). Because of these properties, it is an excellent material for membrane preparation; however, it has a drawback of higher hydrophilicity, which is not acceptable in membranes for water purification. Alumina is nontoxic, highly abrasive, commonly available and economical inorganic material which is widely used in many applications because of its good physical and thermal properties (Saleh et al., 2012). A large variety of solutes such as salts (Demirel et al., 2017; Zhang et al., 2018b), heavy metals (Nayak et al., 2017), carbon ink (Wu et al., 2018), dyes (Ibrahim et al., 2017), bovine serum albumin (Behboudi et al., 2016; Fan et al., 2014; Fang et al., 2017; Zhao et al., 2016), humic acid (Jhaveri et al., 2017) etc. have been used by various researchers to study the effectiveness of PVC based modified composite membranes for various separation applications.

4.2 Materials and Methods

4.2.1 Materials

Polyvinyl chloride (PVC, MW=80000) , nano alumina and humic acid were purchased from Sigma-Aldrich. Polyvinyl Pyrrolidone (PVP) was purchased from HPLC, Mumbai and was used as pore former. N, N-Dimethylacetamide (DMAc) was used as a polymer-solvent and was purchased from Spectrochem, Mumbai. Humic acid powder was purchased from Sigma-Aldrich and diluted with distill water to prepare synthetic wastewater for experiments. Without any further modification and treatment, all chemicals and reagents were used in experiments as purchased.

4.2.2 Preparation of composite membranes

Non-solvent induced phase separation process was adopted for preparing polyvinyl chloride based membranes using alumina nanoparticles for bulk modification in the lab

(Esfahani et al., 2019; Rana et al., 2010). At first, a known amount of alumina was dispersed in DMAc and sonicated for 2 hours to have a homogenous suspension. Then pore former PVP was mixed to the solution and the solution was stirred at room temperature for 2 hours. Subsequently, PVC was added to the solution and mixed by constant stirring for a day until the solution became homogeneous completely. After this solution was further sonicated to remove trapped air bubble in solution and casted with casting knife on a glass plate. After casting the glass plate was immediately immersed in a deionized water bath, which works as non-solvent and phase inversion took place. De-mixing between DI water and DMAc started and polymer PVC was precipitated from the solution and membranes were formed which were easily detached from the plate. During phase inversion, water-soluble PVP was leached out in non-solvent and this created pores within membrane structure. After that, the membrane was immersed in distilled water for 48 hours for complete exchange of solvent. Membranes were dried and stored for further use. In this study, 5 different samples were prepared by varying alumina content (0, 1, 2, 3 and 4%) while keeping polymer amount constant in the polymeric solution. The composition of all membrane samples is given in table 4.1.

Table 4.1: Composition of the membrane samples.

Membrane	DMAc (wt %) Solvent	PVC (wt %) Base Polymer	PVP (wt %) Pore Former	Alumina (wt %) Nano particle
M1	80	19	1	0
M2	79	19	1	1
M3	78	19	1	2
M4	77	19	1	3
M5	76	19	1	4

4.2.3 Characterization methods

The High Resolution scanning electron microscope was used to visualize the morphology of the membrane surface. All the analysis was done using instrument Nova Nano SEM 450, FEI Company of USA (S.E.A.) PTE, LTD. Since the sample is non-metallic, it was coated with gold before observation. Energy-dispersive X-ray spectroscopy (EDS) was used to verify the presence as well as the dispersion of alumina within the membrane. For this purpose Team Pegasus Integrated EDS-EBSD with Octane Plus and Hikari Pro, EDAX USA was used. X-ray diffraction was done to verify the interaction between polymer and alumina particles. Samples were scanned at 2Θ angle from 5-70^{o} . X-ray diffractometer Rigaku Miniflex 600 Desktop X-Ray Diffraction System, RIGAKU Corporation used for analysis was equipped with monochromatic Cu-Kα radiation (λ=0.154 nm). Thermal Gravimetric analysis (TGA) was done to study the thermal stability of membranes using PerkinElmer instrument, Waltham, USA. Composites were heated from room temperature to 500^{o}C at a heating rate of 10^{o}C per minute under a nitrogen atmosphere.

The porosity of membranes was measured by a 24-hour water retention test. Membrane samples of known measurements were soaked in distilled water for one day and after that, samples were taken out and gently wiped on both surfaces by tissue paper and weighed.

After that samples were kept at 50^{o} C in the oven to evaporate the moisture content and again weighed after drying

Porosity is calculated as (Saini et al., 2019)

$$\phi\ (\%) = \frac{W_w - W_D}{\rho_w * V} * 100\% \qquad (4.1)$$

where

W_W and W_D: the weight of the sample in the wet and dry state, V: volume of membrane and $\rho_{w:}$ density of water.

To calculate the mean pore radius of membranes, Guerout–Elford–Ferry (GEF) equation (Behboudi et al., 2016; Hamid et al., 2011; Li et al., 2009; Vatanpour et al., 2012) was used. GEF equation is stated as follows

$$\mathbf{r_m} = \sqrt{\frac{\mathbf{8\eta lQ(2.9 - 1.75\varepsilon)}}{\mathbf{\varepsilon A \Delta P}}} \qquad (\mathbf{4.2})$$

where

η: Viscosity of water; l: Thickness of membrane; Q: Volume of permeate; Ɛ: Porosity of membrane; **Δ**P: Transmembrane pressure; A: membrane area.

Drop shape analyzer DSA25, KRUSSGmbH, Germany was used to know the contact angle of the samples, which eventually shows the hydrophilicity of the membrane. Mean of 4 scans was reported to diminish the scanning errors. Mechanical properties of the membrane, viz. tensile strength and elongation at break were calculated by tensile testing machine (INSTRON 5982 Floor Model System, USA). All the membranes were of size 4 x 1 cm^2, and samples were analyzed at a rate of 1 mm/min using 500 N load cells. All the tests were conducted four times, and the average results were reported.

4.2.4 Performance study and antifouling analysis

Performance of pure PVC membrane and PVC/Alumina composite membrane were further studied on a dead-end lab-scale filtration setup to separate humic acid solution. Flux studies and antifouling analysis of membranes were done using the methodology as discussed in section 3.3.

4.3 Result and discussions

4.3.1 SEM and EDS analysis

Membranes were analyzed by high resolution scanning electron microscope to understand the change in surface morphologies of samples and the results are shown in figure 4.1. An asymmetric pattern of pores can be observed for all the membrane samples. This result is in concurrence with the literature (Rana et al., 2010). During phase inversion when the membranes were immersed in DI water, PVP present in polymeric solution would try to leach into the water. This phenomenon results in formation of asymmetric pores within the membrane structure. It can also be seen by SEM images that the addition of nanoparticles renders the surface look rougher in composite membrane M2 than pure PVC membrane M1. With the addition of alumina, a spherical particle in shape, surface pores looked sharp and clear and almost uniform distribution of alumina particles is also visible on surface.

During phase inversion PVP tends to leach out into the water, but because of polymer-polymer interaction between PVC and PVP, some part of PVP would have remained in polymer matrix, even after keeping the membrane in water for a long time.

When alumina particles were doped into the polymeric solution, it would have also tried to enter into water during phase inversion because of its hydrophilic nature, but PVP here worked as a crosslinker between alumina and PVC, and alumina stayed in polymeric solution. Nanoparticles present in membrane structure created some vicinity around them, and this had resulted in increased porosity, which can be observed in figure 4.1a and 4.1b.

As concentration of alumina was increased in M3-M5 samples, this resulted in more crosslinking between alumina and PVC and higher amount of alumina is visible in images of M3, M4 and M5. As the high amount of nanoparticles came in polymeric

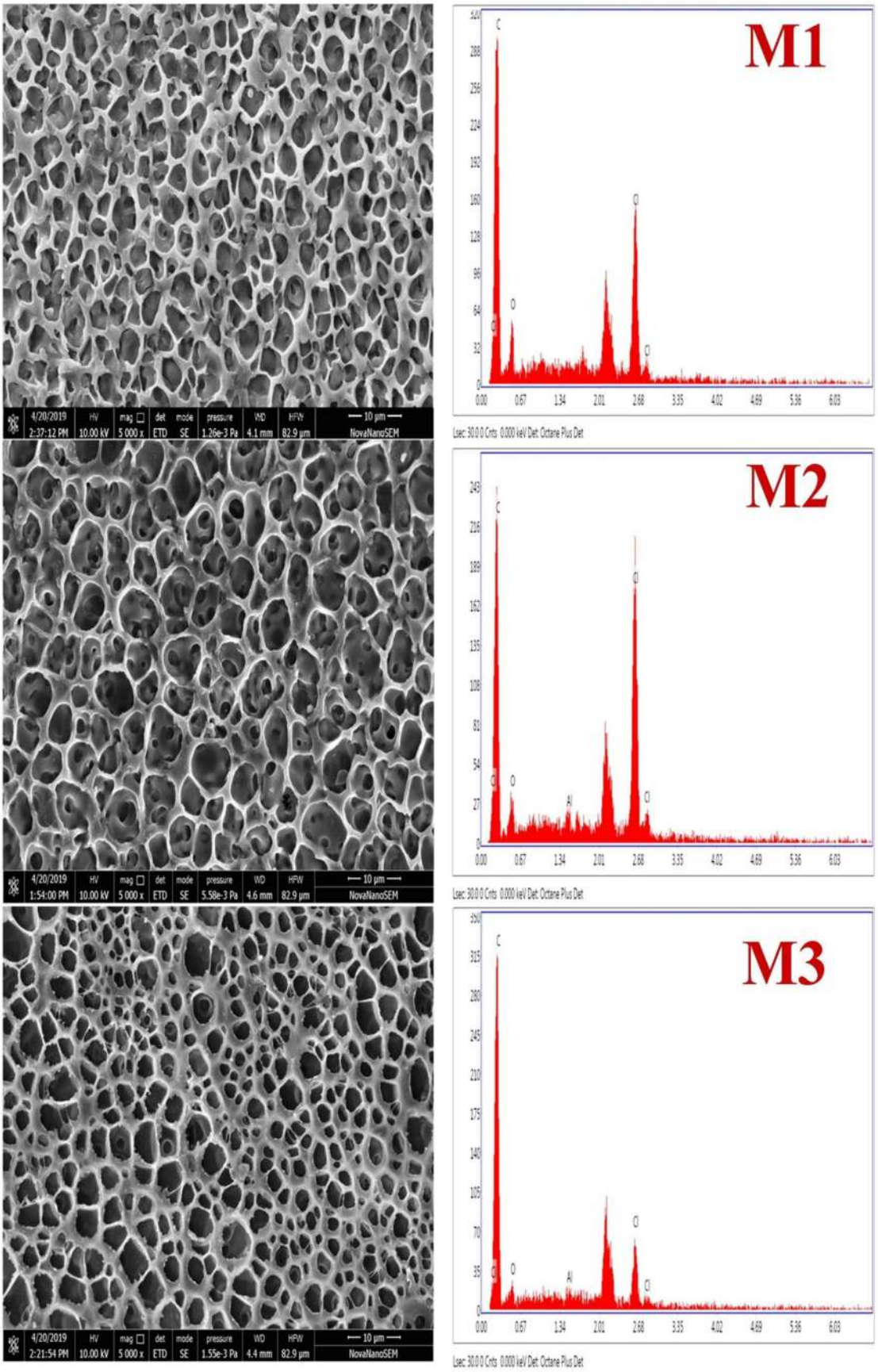

Figure 4.1a: Surface morphology of the top surface of membranes and Energy-dispersive X-ray spectroscopy data for the membrane samples M1-M3.

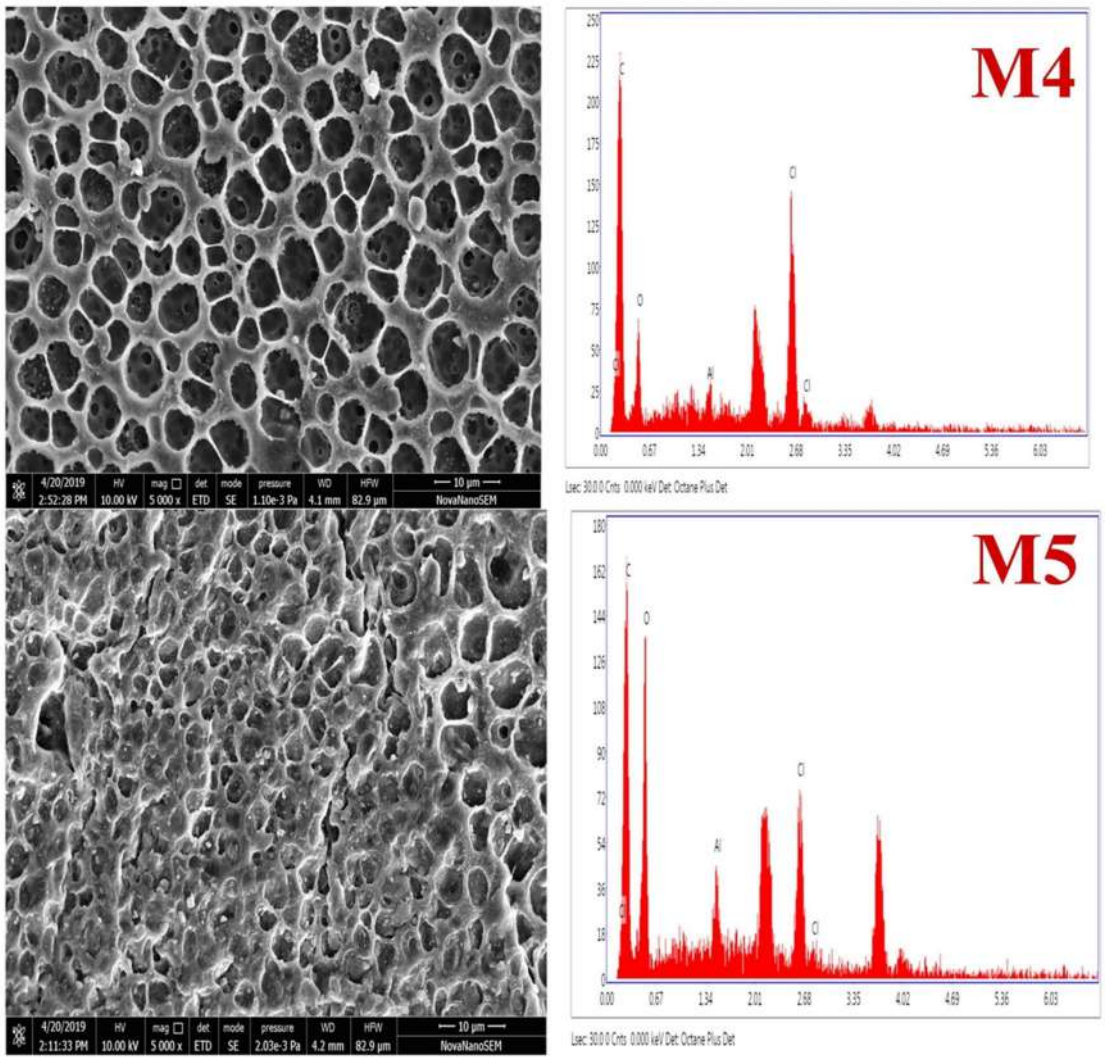

Figure 4.1b: Surface morphology of the top surface of membranes and Energy-dispersive X-ray spectroscopy data for the membrane samples M4 and M5.

solution, agglomeration between the particles took place which affected the porosity of membrane and blocked the membrane surface that could be confirmed from the SEM image of M5 composite membrane. This phenomenon of pore blockage due to particle agglomeration was also reported by some researchers in their study (Behboudi et al., 2016; Demirel et al., 2017; Jhaveri et al., 2017; Li et al., 2009). EDS analysis had verified the presence of alumina in the membrane samples. The weight percentage of alumina was 0.79, 1.24, 2.46, and 3.23 in M2, M3, M4 and M5 composite membranes respectively. Element weight percentage of membrane samples is given in table 4.2.

Table 4.2: Element weight percentage of membrane samples.

Membrane	Element weight (%)			
	C	O	Al	Cl
M1	65.22	10.53	-	24.26
M2	60.82	6.05	0.79	32.34
M3	75.95	7.66	1.24	5.15
M4	60.40	12.82	2.46	25.31
M5	48.13	30.33	3.23	18.31

4.3.2 Thermal Gravimetric analysis

Thermal Gravimetric analysis (TGA) was done to study the change in weight of membrane material with respect to temperature. TGA graphs of unmodified PVC and alumina composite membranes were recorded with a thermal gravimetric analyzer from room temperature to 500^{o}C and the results have been depicted in figure 4.2. For pure PVC membrane as well as composite membranes, a very small fraction of weight about 2.5-3% was observed during primary degradation from room temperature to 140 ^{o}C. For pure PVC membrane M1 secondary and major degradation of material occurred between 140-290 ^{o}C. At the end of this heating zone, pure PVC membrane lost 55.97% weight at 290 ^{o}C while composite membranes M2, M3, M4, and M5 were heated till 304.51, 329.36, 332.65 and 338.12 ^{o}C to lose same weight of material. This behavior was expected because an increase in inorganic content results in high thermal stability of composites. It also verified the interaction between PVC and alumina particles. Almost 63-67% weight was lost by all membranes between 340-360 ^{o}C and membranes showed no significant weight loss between 360-435 ^{o}C. Beyond 435 ^{o}C membrane samples showed a sharp degradation till 500 ^{o}C and 80-83% weight was lost by all membranes. These results showed that composite membranes showed better thermal

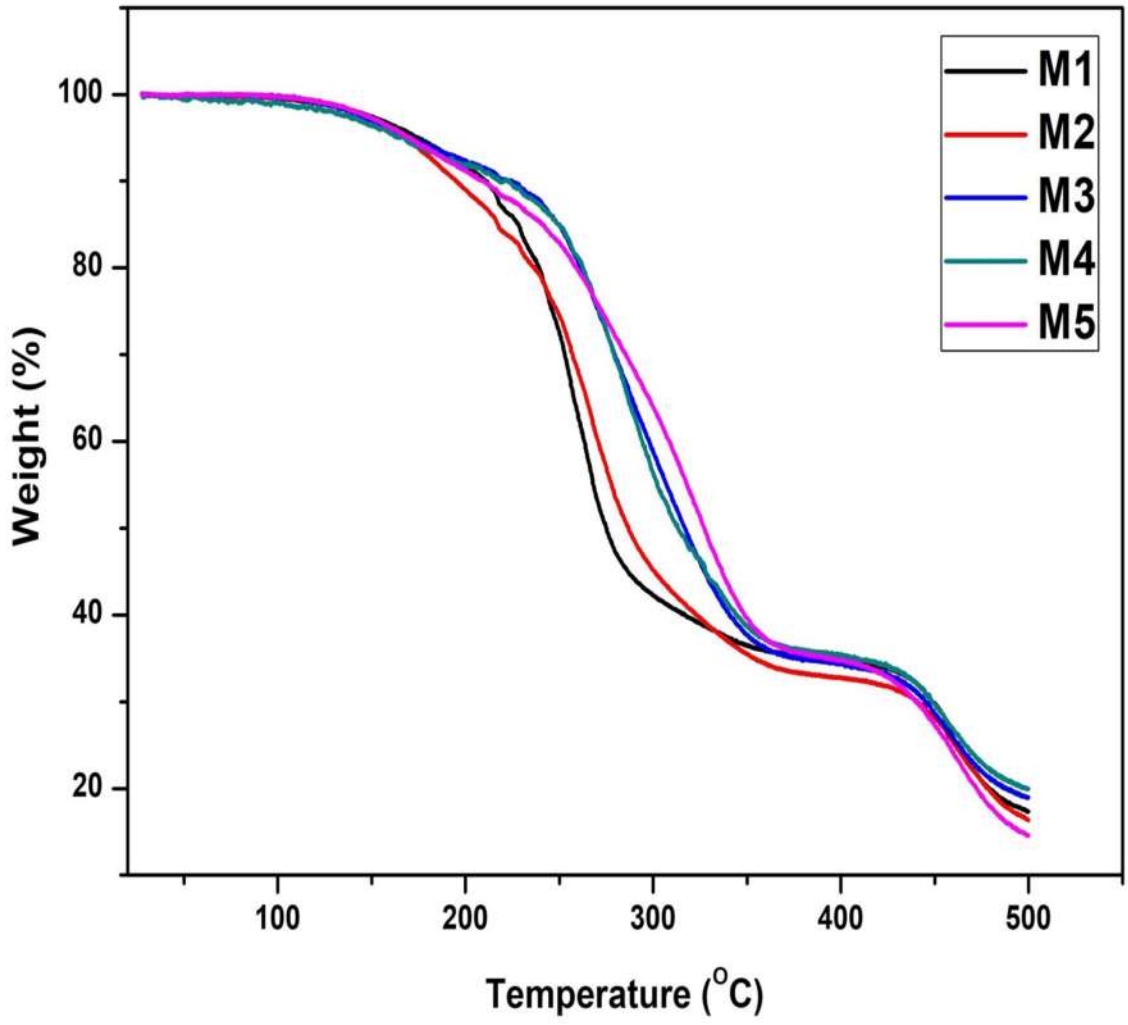

Figure 4.2: Thermal gravimetric analysis of membranes.

stability in major degradation zone because of presence of alumina nanoparticle within membrane structure. Ibrahim et al. (Ibrahim et al., 2017) also reported such three-stage degradation in their study and observed higher thermal stability of polysulfone membrane by blending with zwitterionic nanoparticles.

4.3.3 XRD analysis

XRD patterns of unmodified membrane and composite membranes are presented in figure 4.3. Composite membranes showed wide peaks, which confirm the amorphous nature of composites because membranes were mostly polymer dominant. This

expected amorphous nature of polymeric composites is reported in literature by researchers (Dixit et al., 2019; Jhaveri et al., 2017). Crystalline structure of alumina particles was also seen by XRD.

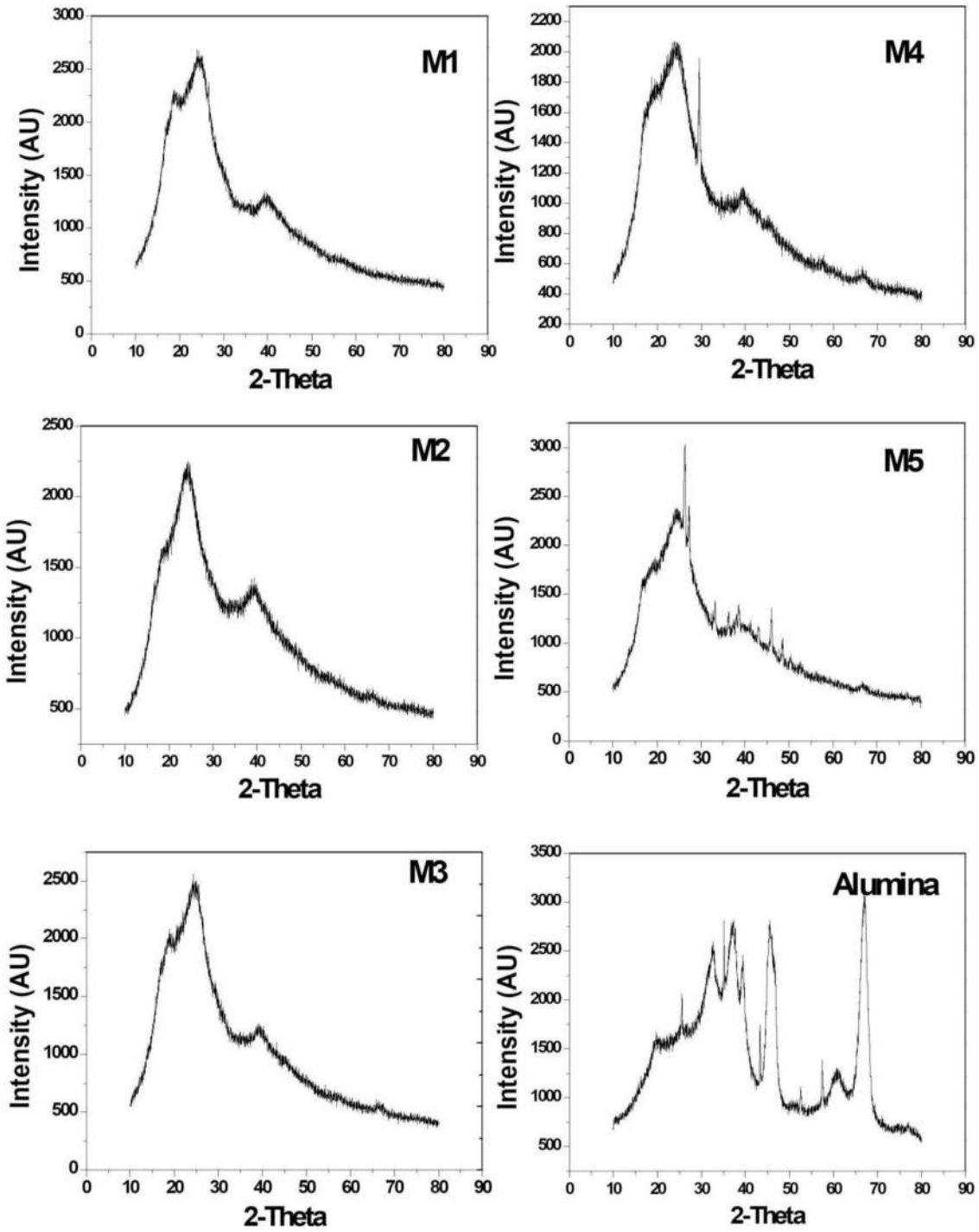

Figure 4.3: XRD patterns of pure PVC membrane, pristine alumina particles and alumina composite membranes M1-M5.

Pure PVC membrane M1 shows 3 major peaks at 18.51^{O}, 24.17 ^{O} and 39.46 ^{O}. In XRD patterns of M2 and M3, new peaks could be observed at 66.34 ^{O} and 66.91 ^{O} respectively. Since XRD gives average intensity of whole structure, addition of alumina does not make any difference in the patterns of M2, M3 membranes as compared to M1. However, the shifting of major peaks is observed. Due to high amount of 3 and 4 weight % in M4 and M5 samples, some new peaks are visible at 29.45 ^{O} in patterns of M4 and 45.98 ^{O}, 48.46 ^{O} in M5. These new peaks correspond to peaks of pure alumina. Changes of values of 2 theta angle and appearance of new peaks verify the interaction between alumina particles and PVC polymer. Major peaks of membrane samples and alumina is shown in table 4.3.

Table 4.3: Major peaks of membrane samples and alumina.

Membrane	Major Peaks (2 Theta)
M1	18.51,24.17,39.46
M2	19.47,24.28,39.43,66.34
M3	18.91,24.53,39.58,66.91
M4	19.43,24.79,29.45,39.43,66.72
M5	19.94,24.58,26.43,27.53,33.28,36.27,39.76,45.98,48.46,66.91
Nano Alumina	19.57,25.48,32.58,35.19,37.24,39.67,43.25,45.43,52.67,57.47,60.76, 66.78

4.3.4 Mechanical Properties

Tensile stress and elongation were tested using a tensile testing machine and the data are given in table 4.4. It can be seen that pure PVC membrane has tensile stress of 66.83 kg/cm^{2,} but as the amount of nanoparticles increases, tensile stress is also enhanced and membrane M5 with 4% of alumina shows highest tensile stress of 87.64 kg/cm^{2}.

4.3.5 Contact angle analysis

Most important property of a membrane is hydrophilicity for the application in aqueous solution. It was observed by the 'drop shape analyzer'. Hydrophilicity depends on the surface roughness, porosity, and materials present within the membrane structure. Lower values of contact angle indicate the more hydrophilic nature of membrane. It was found that addition of nanoparticles affected the hydrophilicity of composite membranes in a positive way. As shown in table 4.4, incorporation of alumina has lowered the contact angle from 73.60 for pure PVC membrane to 44.80 for 4% alumina composite membrane. This shows that the addition of nano alumina has enhanced the hydrophilic nature of the modified membranes.

Table 4.4: Physical and mechanical properties of the membrane samples.

Membrane	Tensile Stress (kg/cm^2)	Elongation at break (%)	Contact Angle (Degree)	Porosity (%)	Mean pore radius(nm)
M1	66.83 (±2.4)	8.62 (±0.7)	73.6 (±3.1)	66.83 (±1.6)	22.4 (±0.8)
M2	70.34 (±2.2)	6.89 (±0.4)	62.2 (±2.2)	68.28 (±2.1)	24.4 (±1.1)
M3	75.53 (±2.7)	6.32 (±0.6)	54.6 (±2.7)	71.83 (±1.9)	26.6 (±1.3)
M4	81.16 (±2.4)	5.52 (±0.5)	52.1 (±1.9)	78.47 (±2.8)	26.4 (±1.1)
M5	87.64 (±3.1)	6.46 (±0.2)	44.8 (±1.5)	75.19 (±1.7)	26.4 (±1.2)

4.3.6 Porosity and Mean pore radius analysis

Porosity was measured by the 24-hour water retention test and it was found that porosity was affected with the incorporation of alumina within membrane structure. The porosity of membrane depends on two factors: (I) pores created by leaching of PVP from polymer solution into water and (II) vicinity created by alumina particles within

the membrane structure around them. As amount of alumina was increased in polymeric solution, more PVP would have retained in the polymeric solution and thus decreasing porosity because of low leaching of PVP into the water. However, at the same time due to vicinity created by alumina within the membrane structure, the porosity increased initially. This effect of increasing porosity was higher than the effect of low leaching. Hence porosity was initially increased in membranes M2, M3, and M4. But due to agglomeration between alumina particles at high weight percentage of alumina, vicinity created by nanoparticles would have decreased, and coarse particles would have also blocked the pores created by leaching of PVP. This would have eventually decreased the porosity of membrane M5, as shown in table 4.4. (Fan et al., 2014) and (Nayak et al., 2017) also observed such change in porosity in their study.

Guerout–Elford–Ferry (GEF) equation was used for calculation of mean pore radius of the membrane, and it was found that all membranes had mean pore radius in the nano range between 22-27 nm. Behboudi et al. have used the same equation and reported mean pore radius in range of 3-7 nm. Similarly (Fan et al., 2014) reported mean pore radius between 14-37 nm by using this equation.

Increase in porosity of composite membranes was because of either enlargement of pores compared to pure PVC membranes or increment of pore numbers within membrane structure Since mean pore radius was almost same in all composite membranes, it is also verified that increment in porosity into the membrane was because of formation of new pores within membrane structure due to presence of alumina particles.

4.3.7 Performance studies

To understand the change in flux for varying concentration of alumina in composite membranes, aqueous solution of humic acid was separated by a lab-scale dead-end

filtration set up. For each membrane sample, flux was calculated in four different situations. First of all, pre-filtration flux J_0 was calculated by passing distilled water only. After the aqueous humic solution was fed to the membrane cell, the permeate flux J_p was estimated for this run. After separation of humic acid solute particles, post-filtration distilled water flux J_1 was calculated. After that the membrane was cleaned by scraping the deposited cake and washing with distilled water and then again distilled water flux (after cleaning) J_2 was calculated. Three different feeds of concentration 10, 20 and 40 mg/L were used to understand the effect of high concentration on the flux. For proper comparison of membrane performance at different feed concentrations, new membranes were used each time for filtering feed of different concentrations. So, here J_0 was common for all three feeds and values of J_P, J_1, and J_2 were different .Hence, there were 10 different flux values for each membrane sample.

As shown in figure 4.4, it was observed in different experimental runs that average flux through composite membranes was higher than pure PVC membrane (M1) with the addition of alumina. Highest flux was observed in the case of pre-filtration distilled water permeation. When membranes were used for the separation of humic acid solution, deposition of solute particles decreased the average flux and value of permeate flux J_P was found lower than J_0.after the separation, when distilled water was again passed through membrane, due to concentration polarization on membrane surface, J_1 was much lower than J_P. After cleaning the membrane when distilled water was again passed through the membrane to know the flux J_2, it was much higher than J_1 as well as J_P but still lesser then J_0. It showed that major decrease in flux is due to reversible fouling, which could be avoided by membrane cleaning.

In each membrane sample, similar patterns of fluxes J_0, J_P, J_1 and J_2 were found. It was observed that addition of alumina increased the average flux for each condition in the

composite membrane. It was highest in the case of membrane M4, almost 200% higher than pure PVC membrane M1. Changes in flux depend on the membrane porosity as well as hydrophilicity of membrane (Cao et al., 2006; Rabiee et al., 2015). It can be observed from values listed in table 4.2 that the porosity does not change much for the composite membranes of varying composition. So, it could be estimated that major change in flux was due to improved hydrophilicity in composite membranes. Higher hydrophilicity helps in easy permeation of water through the membrane (Leo et al., 2012). Similar flux patterns were found in the case of high concentration feed of 20 and 40 mg/L with a change that in those cases, values of fluxes J_P, J_1 and J_2 were found lower than the 10 mg/L concentration feed because of thick cake layer formation on membrane surface due to presence of higher amount of solutes in feed (Younas et al., 2018).

4.3.8 Fouling parameter study

Fouling ratio is a unitless parameter which gives information that how the performance of a membrane drops during filtration and is expressed as reversible fouling, irreversible fouling and total fouling (Behboudi et al., 2016). Values of these parameters were calculated using equation 3.4, 3.5 and 3.6 and have been plotted in figure 4.5. A significant change was observed in fouling ratios of composite membranes with presence of alumina particles. It was seen that total fouling was lowest in case of membrane M4, however as the feed concentration was increased, fouling was also increased. From figure 4.5 it can be assessed that reversible fouling has a larger share of total fouling in the membrane. It was about 68-77% of total fouling in various cases.

Absolute values of reversible fouling were also observed to be higher at higher feed concentration, which showed that some small pores were blocked more easily in the presence of high amount of solute in feed and at high concentration feed conditions total

fouling was dominated by irreversible fouling. In all feed conditions, M4 showed the lowest fouling across membrane. For M4 membrane irreversible fouling were 2.78, 6.96, and 11.33 % for 10, 20 and 40 mg/L feed concentrations respectively.

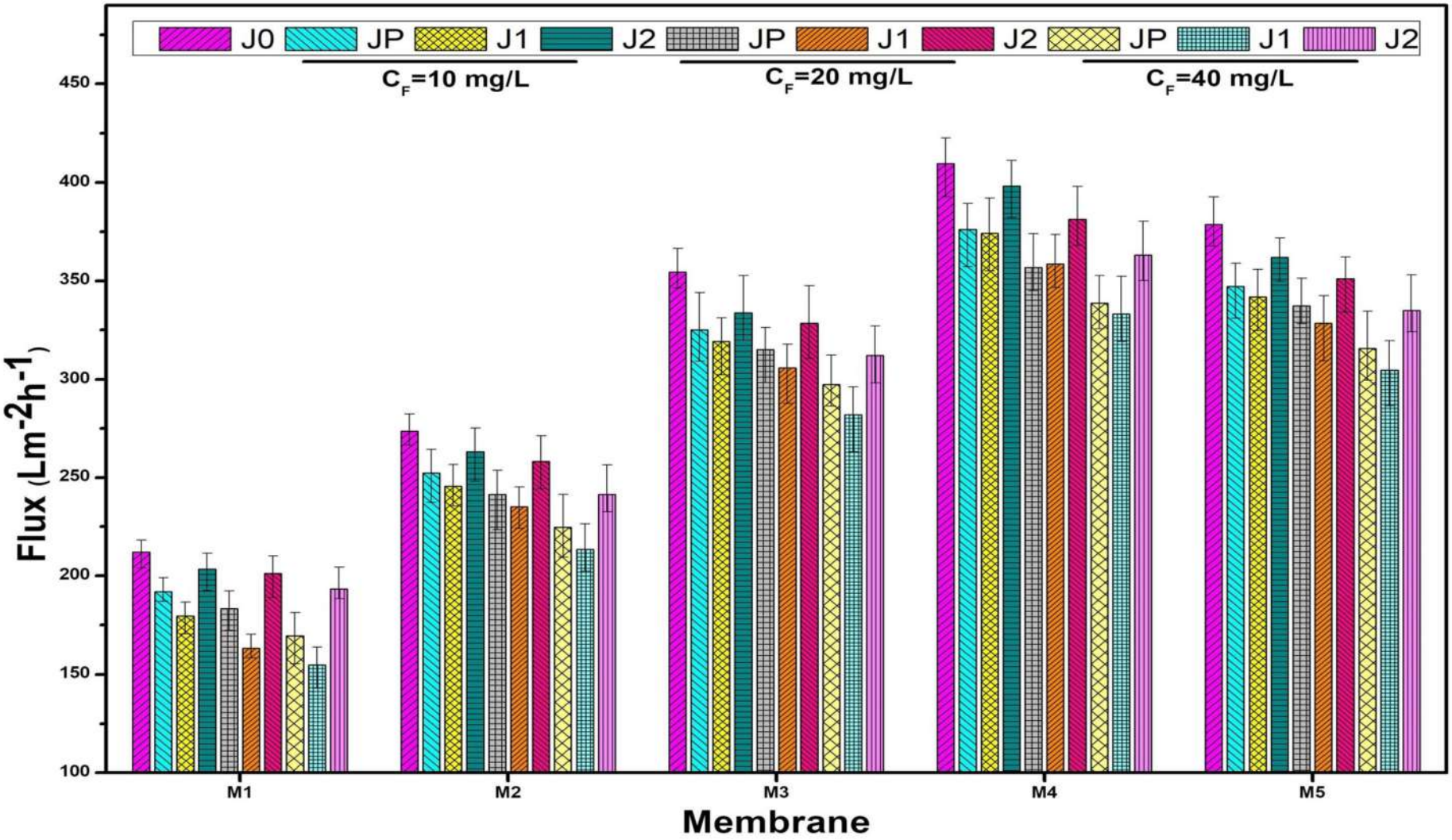

Figure 4.4: Pure water fluxes and permeates flux for feed conditions 10mg/L, 20mg/L and 40 mg/L Humic acid solution.

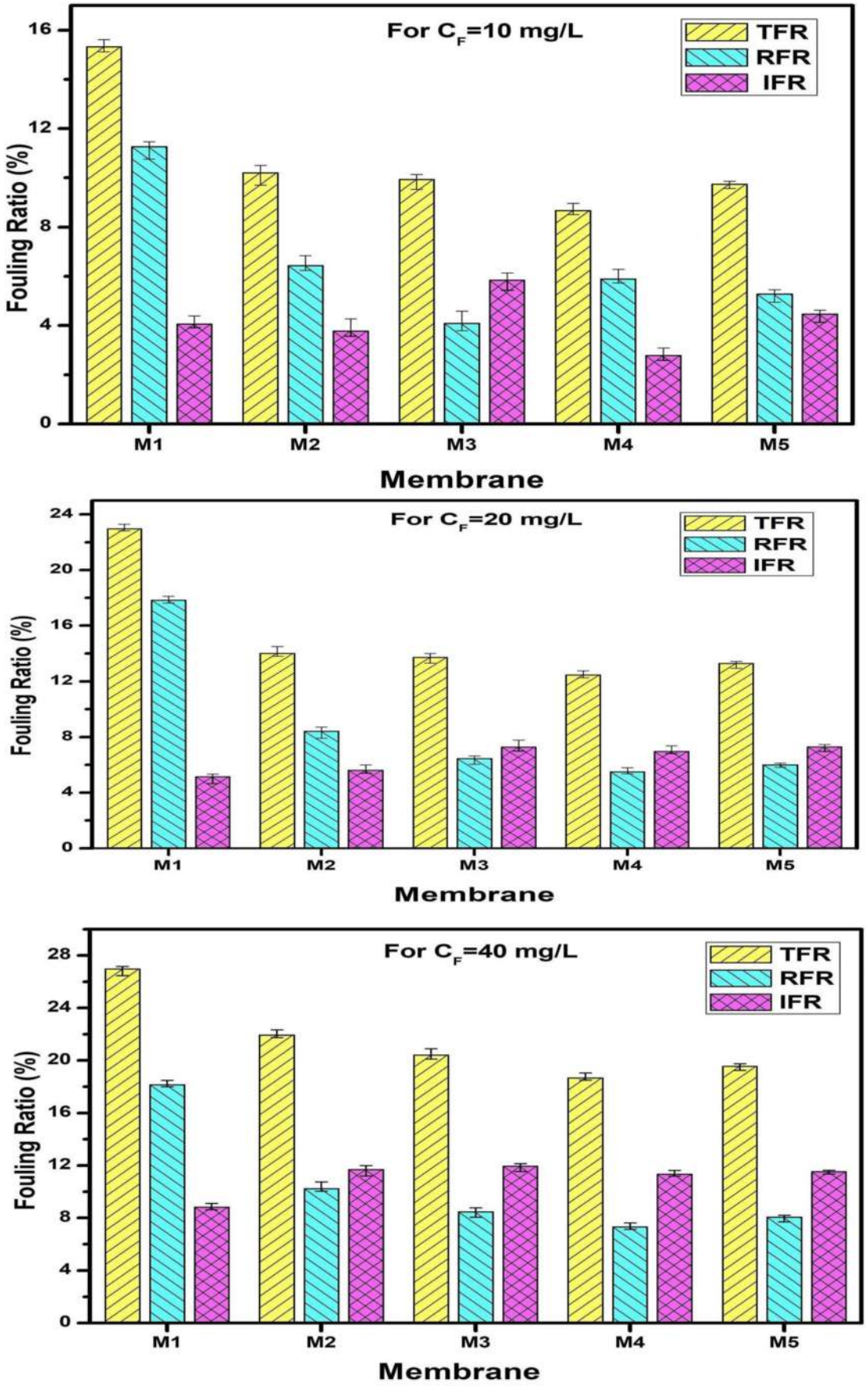

Figure 4.5: Fouling ratio for 10 mg/L, 20 mg/L and 40 mg/L Humic acid solution.

4.3.9 Rejection rate

Rejection denotes the efficiency of membrane to retain the part of solute present in feed. It was calculated by equation 3.12 and has been plotted in figure 4.6. Pure PVC membrane M1 showed highest rejection in all feed conditions. For feed of 10 mg/L concentration, rejection was 95.7%. However it changed with high solute present in feed at higher feed conditions (Jafarzadeh et al., 2015; Rabiee et al., 2015).

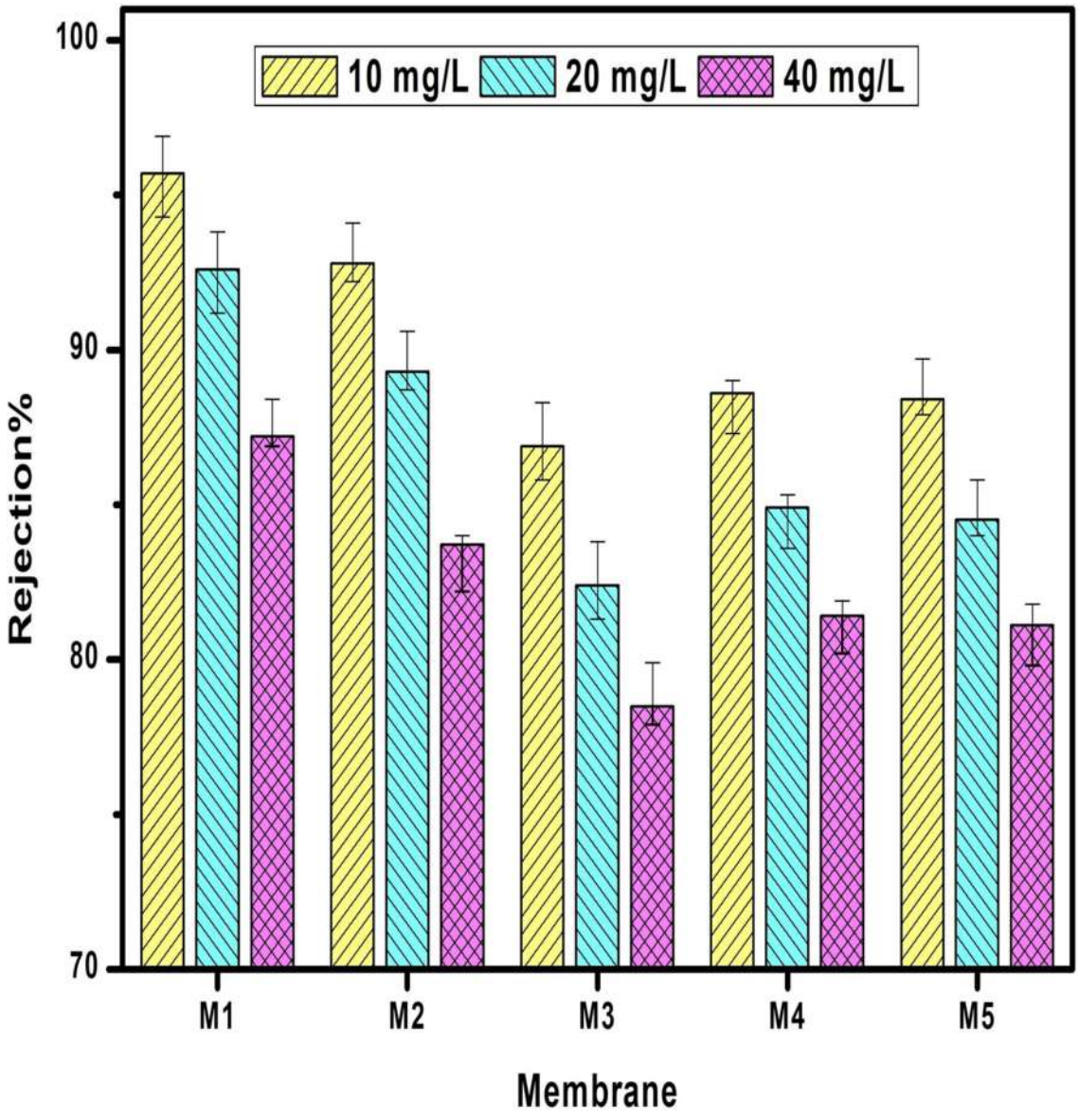

Figure 4.6: Rejection for 10 mg/L, 20 mg/L and 40 mg/L Humic acid solution.

4.3.10 Flux recovery

Flux recovery is another parameter to express membrane's antifouling nature. It gives information about how much of initial flux was recovered after cleaning of membrane. Almost 85-95% of membrane flux was recovered after cleaning of membrane as shown in figure 4.7. Since fouling was higher at high feed concentration, flux recovery was also less (Jafarzadeh et al., 2015). Flux recovery was highest for composite PVC membrane M4.

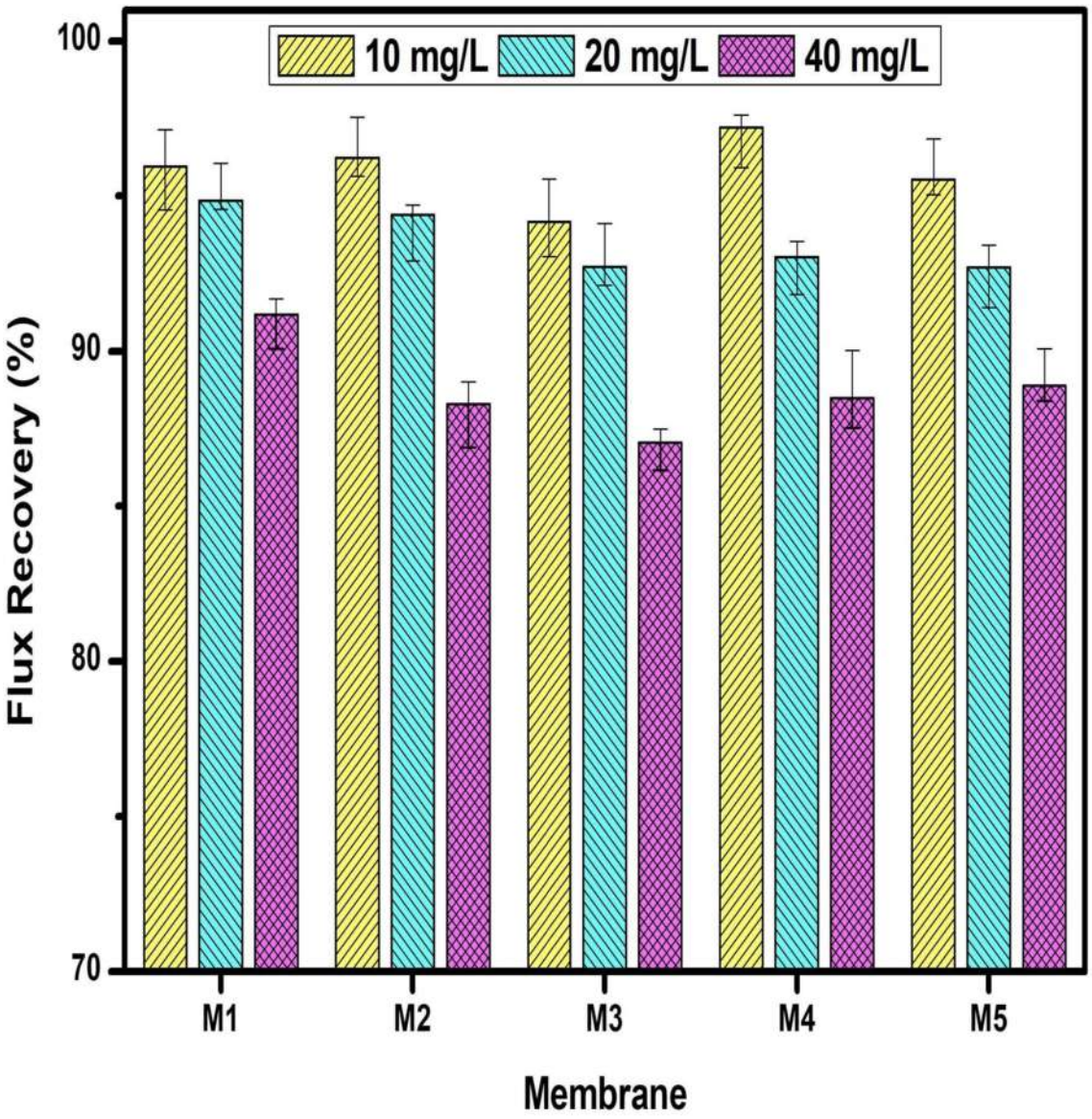

Figure 4.7: Flux Recovery for 10 mg/L, 20 mg/L and 40 mg/L Humic acid solution.

4.3.11 Relative Flux

Relative flux is also a antifouling parameter to observe how flux varies through a membrane when it is subjected to real operation as compared to pure water flow. This is a fractional value and ratio of flux of humic acid solution to pure water flux (Maximous et al., 2009). As it is shown in figure 4.8, for 10 mg/L solution relative flux varies between 0.90-0.92. But as the amount of humic acid was increased in feed, flux through the membrane decreased because of various resistances provided by membrane and cake layer to the flow. As it is shown in figure 4.8, that for the 40 mg/L feed solution, relative flux was lowest for membrane M1 but as the concentration of alumina increased in composite membrane, there was an improvement of relative flux which shows that lower drop in flux is observed at high solute concentrations in composite membranes.

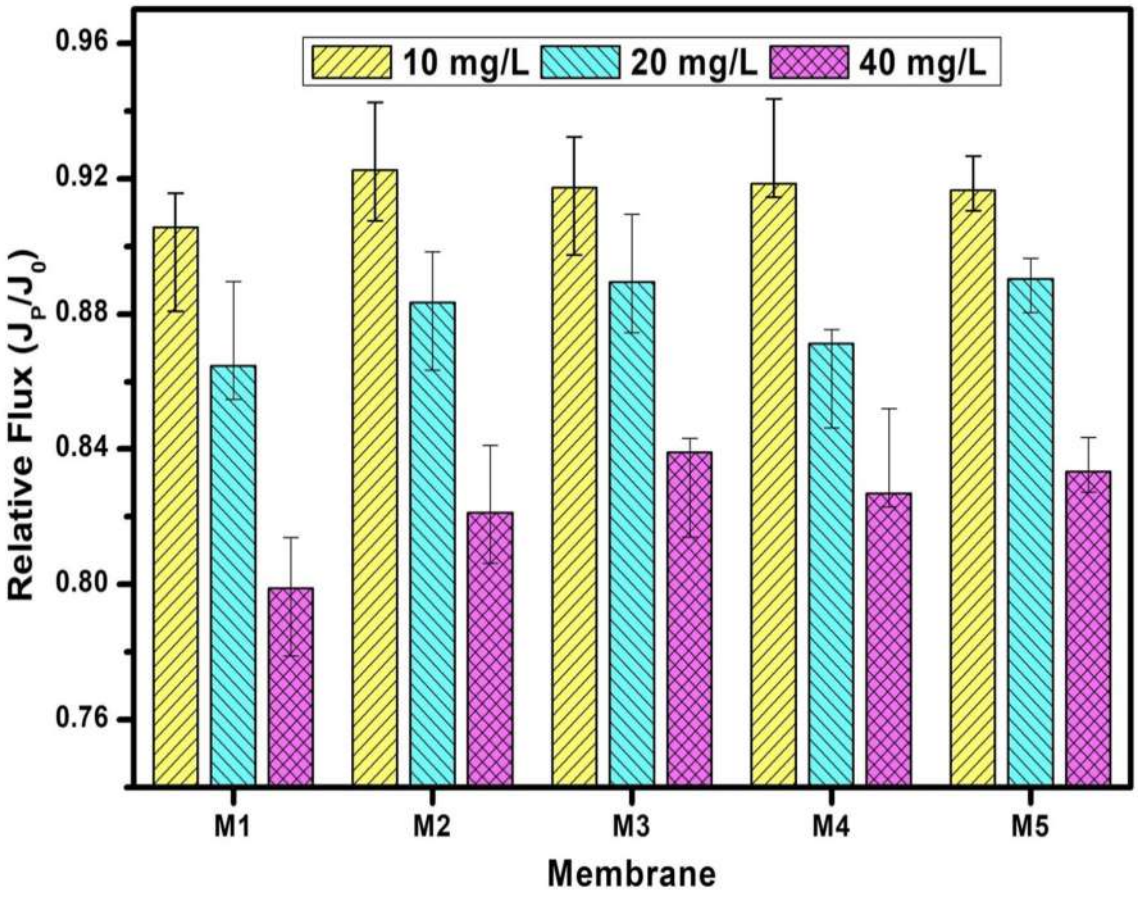

Figure 4.8: Relatives flux of the membranes for 10 mg/L, 20 mg/L and 40 mg/L Humic acid solution.

4.3.12 Membrane resistance

During the separation, resistance to the separation is also experienced, which can be used to express antifouling nature of membrane (Li et al., 2017; Rajesha et al., 2019). This resistance is made of three fractions viz. membrane intrinsic resistance, irreversible fouling resistance, and resistance due to concentration polarization. However, intrinsic membrane resistance had major role in total resistance and rest in minute fraction as compared to total resistance. By figure 4.9, it can be observed that irreversible fouling resistance and resistance due to concentration polarization increased with higher feed concentration and it increased the total resistance to separation. Membrane M4 showed lowest resistance to separation in all three feed conditions. Younas et al. (Younas et al., 2016) had also discussed the effect of resistance to discuss antifouling nature of membranes.

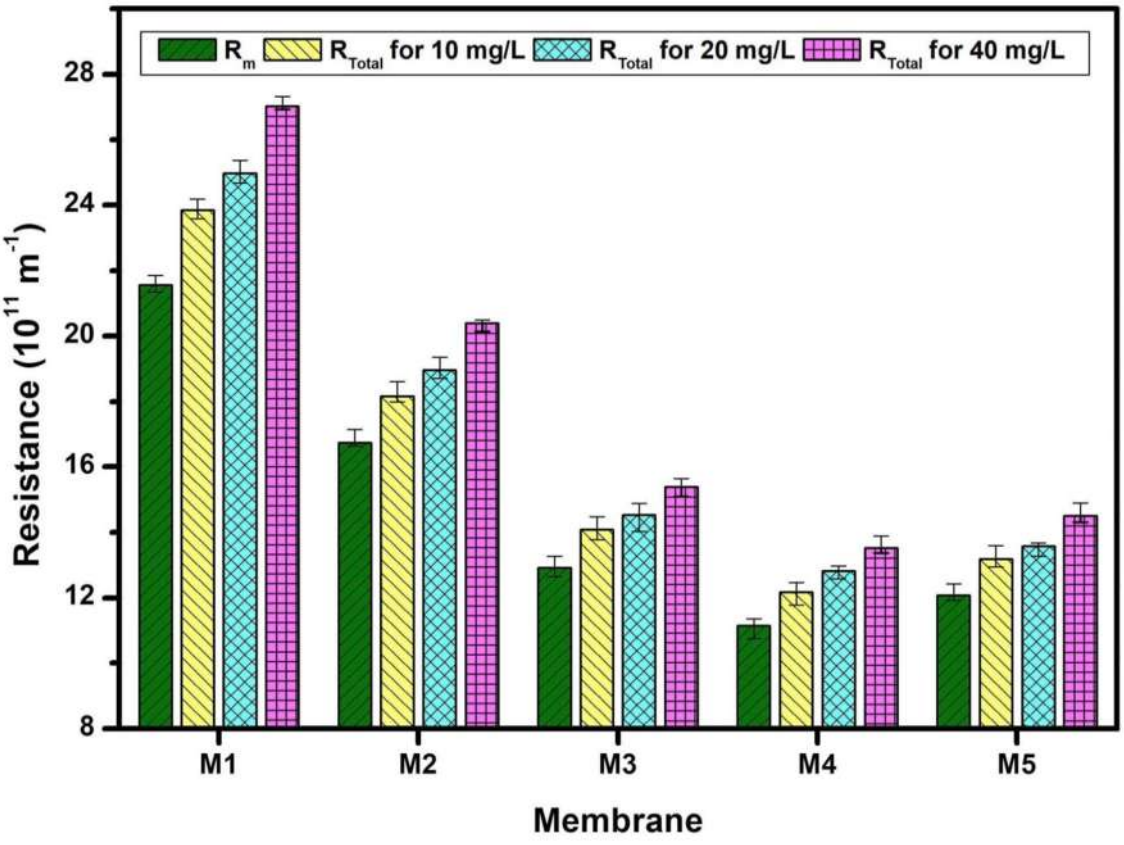

Figure 4.9: Intrinsic and total resistance to membranes for 10 mg/L, 20 mg/L and 40 mg/L Humic acid solution

4.4 Conclusions

PVC based membranes were prepared using different concentration of nano alumina and the resulting changes that occurred in their chemical and physical properties were studied. Hydrophilicity of composite membranes was improved and it was highest for 4 % alumina composite. By SEM analysis, it was observed that the surface morphology of membranes changed, and the porosity of membranes had a decreasing trend due to crosslinking of polymer and high dose of inorganic particles. EDS analysis verified the presence of nanoparticle in the membrane. By XRD, it was observed that polymeric membranes generally possess amorphous nature, and sometimes it shifts to a semi-crystalline phase with the addition of inorganic nanoparticle. Tensile strength of composite membranes was increased by addition of nanoparticles. Water retention test was done to measure porosity. Highest porosity was found to be 78.47% for 3% alumina composite. Mean pore radius was calculated using GEF equation and all the membranes had pores in nano range (22-27 nm).

Membrane flux increased with the presence of nanoparticles, and highest flux was 409.6 L/m^2h for 3% PVC/Alumina membrane. As the solute concentration in feed was increased, the flux declined. Total fouling was effected by varied concentration of Nanoparticles, and it was lowest for 3% PVC/Alumina membrane. Fouling increased for higher feed concentration. Flux recovery was 97.22 for 3% PVC/Alumina membrane at 10 mg/L feed. Highest rejection was observed for 10 mg/L feed, and it was 95.7% for 3% PVC/Alumina membrane. It also dropped with higher feed concentration. Total resistance to separation due to membrane, irreversible fouling, and concentration polarization was also affected, and it was lowest for 3% PVC/Alumina membranes.